Hydropower Plants Modelling for Monitoring Purposes

Augustin Alonso, Gerard Robert, Gildas Besançon, Roland Hildebrand

Hydropower Plants Modelling for Monitoring Purposes

Augustin Alonso [*,**] **Gerard Robert** [**] **Gildas Besançon** [*] **Roland Hildebrand** [***]

[*] *Univ. Grenoble Alpes, GIPSA-lab, F-38000 Grenoble, France (e-mail: augustin.alonso@grenoble-inp.fr, gildas.besancon@grenoble-inp.fr)*
[**] *EDF, Hydro Engineering Centre, Savoie Technolac, F-73373 Le Bourget du Lac, France (e-mail: augustin.alonso@edf.fr, gerard.robert@edf.fr)*
[***] *Univ. Grenoble Alpes, LJK, F-38000 Grenoble, France (e-mail: roland.hildebrand@univ-grenoble-alpes.fr)*

Abstract: In this paper, a direct hydromechanical modelling approach is proposed for hydropower plants, capturing their main characteristics via a few physical parameters of industrial interest. A kinetic model is developed and compared to the standard mechanical model while some parameters are estimated using an instrumental variable method. The model is finally validated with industrial data, showing a good consistency between real behaviors and simulated ones.

Keywords: Modeling and simulation of power systems, Power and Energy Systems, Digital twins for power and process systems

1. INTRODUCTION

Hydropower plants are the main source of renewable electricity in the world. For monitoring and predictive maintenance purposes, it is useful to have a digital twin based on a physical hydromechanical model involving constant or varying meaningful parameters. Using such a model indeed, combined with sensor data, can help engineers to diagnose the state of the plant and provide early fault detection (increase of head losses in the tunnel and penstock, bearing, actuator or sensor failure, turbine erosion, presence of a foreign object in the turbine, cavitation phenomenon).

Physical modelling ingredients can be found in various references, such as Munoz-Hernandez et al. (2012) and Robert and Besançon (2019). The recent review Ozkaya and Kosalay (2018) on system identification for various power generation systems includes hydropower case, but with black-box, or grey-box, approaches. References De Jaeger et al. (1994) and Gracino et al. (2021) instead provide some physical-based identification studies, but with pretty simplified models.

In the same spirit of tractable models, the main objective of this article is to fully re-derive and validate a physical model for a hydroelectric power plant, usable to estimate some of its physical parameters of interest for its monitoring (coefficients of head losses, efficiency of the turbine, inertia constant of the generating unit), from commonly available industrial measurements. The modelling approach which is considered here relies on underlying mechanics and hydraulics, while validation is achieved on the basis of real industrial data collected on plants from EDF group (the main French electric utility company). For such data, illustrative simulation results are provided.

The paper is organized as follows: the proposed modelling approach is first developed in section 2 and its validation based on industrial data is then presented in section 3. Some conclusions finally end the paper in section 4.

2. PROPOSED MODELLING APPROACH

2.1 Mechanical Model

The power balance diagram (valid for all speeds) presented in Fig. 1. summarizes the intermediate powers between the hydraulic power and the electrical power supplied by the alternator. The power absorbed by the rotor is not shown because it is immediately dissipated by Joule effect. In our assumptions, we choose to neglect the friction losses in the flanges, the iron losses and the copper losses in the stator.

Let us set:

- ω^*, ω_0 the angular electrical velocities of the rotor and synchronism, $rad.s^{-1}$ ($\omega_0 = 2\pi f_0 = 100\pi\ rad.s^{-1}$, f_0 represents the nominal frequency of the network).
- n_p the number of pole pairs of the rotor.
- Ω, Ω_0 the angular mechanical velocities of the rotor and synchronism, $rad.s^{-1}$.

The angular velocities are related with each other:

$$\omega^* = n_p \Omega \tag{1}$$

$$\omega_0 = n_p \Omega_0 \tag{2}$$

The normalized angular velocity (in p.u.) is then defined:

$$\omega = \frac{\omega^*}{\omega_0} = \frac{\Omega}{\Omega_0} \tag{3}$$

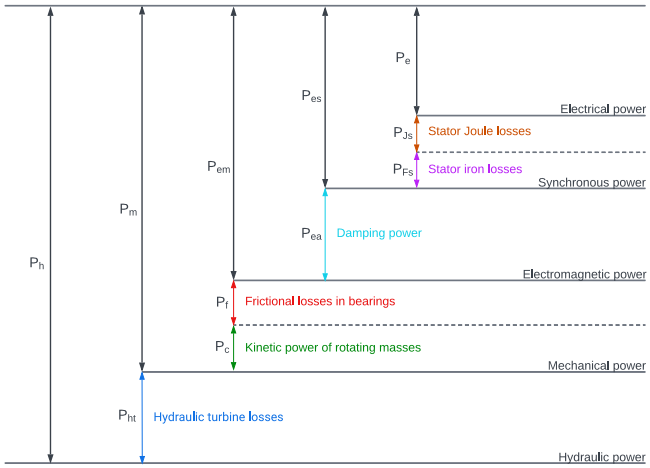

Fig. 1. Power diagram

The fundamental principle of dynamics, applied to a rotating mass, gives the equation of motion of the generating unit shaft (see Bergen and Vittal (2000), page 533):

$$J\dot{\Omega} = C_m - C_{em} - C_f \tag{4}$$

with:

- J the momentum of inertia of rotating masses (rotor and turbine), $kg.m^2$.
- C_m the mechanical torque on the shaft line, $N.m$.
- C_{em} the electromagnetic torque of the synchronous machine, $N.m$.
- C_f the friction torque generated in the bearings, $N.m$.

In our assumptions, the friction torque is neglected.

As for the electromagnetic torque C_{em}, it can be decomposed (see Barret (1987) pages 151-152) into a synchronous torque C_{es} $(N.m)$ and an asynchronous torque C_{ea}, $N.m$ (referenced to a fictitious reference frame rotating at the synchronism speed):

$$C_{em} = C_{es} + C_{ea} \tag{5}$$

where C_{ea} corresponds to some damping D_0 $(N.m.s)$ as:

$$C_{ea} = D_0(\Omega - \Omega_0) \tag{6}$$

Thus we have:

$$J\dot{\Omega} = C_m - C_{es} - D_0(\Omega - \Omega_0) \tag{7}$$

On the other hand, the mechanical power P_m supplied by the turbine (W) and the synchronous electromagnetic power of the alternator P_{es} (W) satisfy:

$$P_m = C_m\Omega, \;\; P_{es} = C_{es}\Omega \tag{8}$$

From Figure 1 we also have:

$$P_{es} = P_e + P_{Fs} + P_{Js} \tag{9}$$

where P_e is the electrical power produced by the alternator (W), and P_{Fs}, P_{Js} are power losses related to iron and copper losses respectively, which will be here neglected. Namely:

$$P_{es} \approx P_e \tag{10}$$

Now multiplying equation (7) by Ω, we obtain:

$$J\Omega\dot{\Omega} = C_m\Omega - C_{es}\Omega - D_0\Omega(\Omega - \Omega_0) \tag{11}$$

which gives according to (3), (8) and (10):

$$J\Omega_0^2\omega\dot{\omega} = P_m - P_e - D_0\Omega_0^2\omega(\omega - 1) \tag{12}$$

Let E_c be the kinetic energy of rotating masses:

$$E_c = \frac{1}{2}J\Omega^2 \tag{13}$$

It can be normalized into:

$$e_c = \left(\frac{\Omega}{\Omega_0}\right)^2 = \omega^2 \tag{14}$$

then giving:

$$\dot{e_c} = 2\omega\dot{\omega} \tag{15}$$

By also normalizing the powers as:

$$p_m = \frac{P_m}{S_n}, \;\; p_e = \frac{P_e}{S_n} \tag{16}$$

for S_n the apparent rated power of the alternator (VA), we obtain:

$$\frac{J\Omega_0^2}{S_n}\omega\dot{\omega} = p_m - p_e - \frac{D_0\Omega_0^2}{S_n}\omega(\omega - 1) \tag{17}$$

Let us set:

$$H_c = \frac{J\Omega_0^2}{2S_n} \quad \text{and} \quad D = \frac{D_0\Omega_0^2}{S_n} \tag{18}$$

where H_c represents the inertia constant of the generating unit, then:

$$2H_c\omega\dot{\omega} = p_m - p_e - D(\omega^2 - \omega) \tag{19}$$

and from (14) and (15):

$$H_c\dot{e_c} = p_m - p_e - D(e_c - \sqrt{e_c}) \tag{20}$$

Considering now the hydraulic power P_h (W) and the efficiency of the turbine $\eta = \eta(\omega, h, q) \approx \eta(h, q)$ (for ω close to 1 and h and q defined in section 2.2), we have the following identity, and normalization:

$$P_m = \eta P_h; \quad p_h = \frac{P_h}{S_n} \tag{21}$$

Finally, the mechanical model, which can be called kinetic model, can be described by the following first order state-space representation:

$$\begin{cases} H_c\dot{e_c} = \eta p_h - p_e - D(e_c - \sqrt{e_c}) \\ \omega = \sqrt{e_c} \end{cases} \tag{22}$$

Notice that this model is consistent with the more standard one as it can be found in Machowski et al. (2020) (p. 195) for instance, and written as:

$$M\dot{\omega} = p_m - p_e - D(\omega - 1) \tag{23}$$

for some M.

Model (23) can indeed be recovered from equation (19) by dividing it by ω and considering an approximate linearization of the equation around $\omega = 1$ (also corresponding to powers $p_m = p_e$), that is for Ω close to Ω_0.
In that case indeed, equation (23) is directly obtained, with:

$$M = 2H_c = \frac{J\Omega_0^2}{S_n} \tag{24}$$

2.2 Hydraulic Model

In order to clarify hydraulic power p_h in equation (22), let us now consider the hydraulic part of the hydropower plant. Figure 2 represents the hydraulic configuration of a single penstock scheme with k immersed turbines (Francis type).

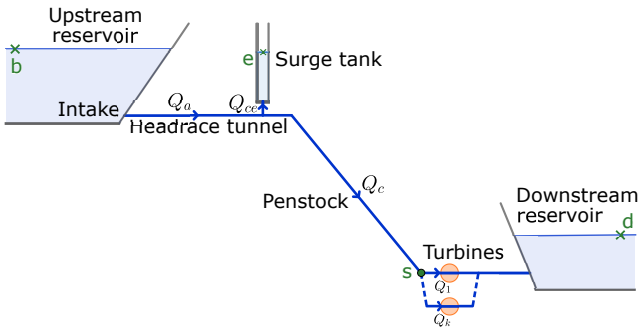

Fig. 2. Hydroelectric power plant layout

In this study, we consider the generating unit n°i turbining/pumping a flow rate $Q = Q_j,\ j \in [1, k]$.

We define the set of points $\mathcal{A} = \{b, e, s, d\}$ as shown in Figure 2, and the following notations:

- Q_a, Q_{ce}, Q_c the flow rate in the headrace, the surge tank and the penstock, respectively, $m^3.s^{-1}$;
- Q_j $(1 \leq j \leq k)$ the flow rate turbined/pumped by the j^{th} generating unit, $m^3.s^{-1}$;
- K_a, K_c the coefficient of head losses in the headrace tunnel and the penstock respectively;
- L_a, L_c the length of the headrace tunnel and the penstock, respectively, m;
- S_a, S_e, S_c the cross-section surface of the headrace tunnel, surge tank and penstock, respectively, m^2;
- $Z_i (i \in \mathcal{A})$ the height of the point i, in reference to the altitude of the minimum operating surface point of the lower reservoir, m;
- P^r_{atm} the atmospheric pressure at points (b, e, d), Pa;
- P^r_s the ambiant pressure at point s, Pa;
- ρ the water density ($\approx 1000\ kg.m^{-3}$);
- g the acceleration due to gravity ($\approx 9.81\ m.s^{-2}$).

We clearly have:

$$Q_c = \sum_{j=1}^{k} Q_j,\ Q_a = Q_c + Q_{ce} \tag{25}$$

It is assumed that:

- Water is an incompressible fluid.
- The penstock is inelastic.
- The regular head losses of the two reservoirs are negligible.
- The head losses in the surge tank and the branches are neglected (a branch is the junction between a penstock and a turbine).
- The generating units can operate in turbine or pump mode (the units can be reversible).
- The kinetic terms (of the form $\frac{V^2}{2g}$ for a velocity V) in the reservoirs are neglected.

By applying generalized Bernoulli's principle to the non-permanent flows (see Robert and Michaud (2017)) between the upper reservoir (point b in Fig. 2) and the surge tank (point e in Fig. 2), we get:

$$Z_b + \frac{P^r_{atm}}{\rho g} = Z_e + \frac{P^r_{atm}}{\rho g} + K_a|Q_a|Q_a + \frac{L_a}{S_a g}\dot{Q}_a \tag{26}$$

Let us set:

$$\alpha_a = \frac{L_a}{S_a g}, \text{the inertia coefficient of the headrace tunnel.} \tag{27}$$

Then:

$$\alpha_a \dot{Q}_a = Z_b - Z_e - K_a|Q_a|Q_a \tag{28}$$

Let us now apply generalized Bernoulli's principle to the non-permanent flows between the surge tank (point e) and the penstock separation point (point s), this yields:

$$Z_e + \frac{P^r_{atm}}{\rho g} = Z_s + \frac{P^r_s}{\rho g} + \frac{{V_s}^2}{2g} + K_c|Q_c|Q_c + \frac{L_c}{S_c g}\dot{Q}_c \tag{29}$$

where:

$$V_s = \frac{Q_c}{S_c} \tag{30}$$

With notations:

$$\alpha_c = \frac{L_c}{S_c g}, \quad \beta_c = \frac{1}{2g{S_c}^2}, \quad H_s = \frac{P^r_s - P^r_{atm}}{\rho g} \tag{31}$$

Wet get:

$$\alpha_c \dot{Q}_c = Z_e - Z_s - H_s - \beta_c {Q_c}^2 - K_c|Q_c|Q_c \tag{32}$$

We can again apply generalized Bernoulli's principle to the non-permanent flows now between the surge tank (point e) and the downstream reservoir (point d):

$$Z_e + \frac{P^r_{atm}}{\rho g} = Z_d + \frac{P^r_{atm}}{\rho g} + K_c|Q_c|Q_c + \alpha_c \dot{Q}_c + H \tag{33}$$

where H denotes the net head height (the counter-electromotive force generated by the hydraulic unit), in m.

Hence:

$$H = Z_e - Z_d - K_c|Q_c|Q_c - \alpha_c \dot{Q}_c \tag{34}$$

Using generalized Bernoulli's principle once more between the penstock separation point (point s) and the downstream reservoir (point d) further gives:

$$Z_s + \frac{P^r_s}{\rho g} + \frac{{V_s}^2}{2g} = Z_d + \frac{P^r_{atm}}{\rho g} + H \tag{35}$$

that is:

$$H = Z_s - Z_d + H_s + \beta_c {Q_c}^2 \tag{36}$$

Neglecting the role of the surge tank ($Q_{ce} = 0$), it is possible to apply generalized Bernoulli's principle to the non-permanent flows between the upstream reservoir (point b) and the downstream reservoir (point d):

$$\begin{aligned} Z_b + \frac{P^r_{atm}}{\rho g} = Z_d + \frac{P^r_{atm}}{\rho g} + K_a|Q_a|Q_a + K_c|Q_c|Q_c \\ + \alpha_a \dot{Q}_a + \alpha_c \dot{Q}_c + H \end{aligned} \tag{37}$$

Notice that when $Q_{ce} = 0$, we have $Q_a = Q_c$, and thus:

$$H = Z_b - Z_d - K|Q_c|Q_c - \alpha \dot{Q}_c \tag{38}$$

with:

$$K = K_a + K_c,\ \alpha = \alpha_a + \alpha_c \tag{39}$$

However, the water level in the surge tank can be modelled by the following equation:

$$S_e \dot{Z}_e = Q_a - Q_c \tag{40}$$

Combining equations (28), (32) and (40), we obtain the following state model:

$$\begin{cases} \alpha_a \dot{Q}_a = Z_b - Z_e - K_a |Q_a| Q_a \\ \alpha_c \dot{Q}_c = Z_e - Z_s - H_s - \beta_c {Q_c}^2 - K_c |Q_c| Q_c \\ \dot{Z}_e = \dfrac{Q_a - Q_c}{S_e} \end{cases} \tag{41}$$

Let us normalize the involved quantities as follows:

$$z_i = \frac{Z_i}{H_{max}} (i \in \mathcal{A}) \tag{42}$$

$$h = \frac{H}{H_{max}},\ h_s = \frac{H_s}{H_{max}} \tag{43}$$

$$q_a = \frac{Q_a}{Q_{c_{max}}},\ q_c = \frac{Q_c}{Q_{c_{max}}} \tag{44}$$

$$K_a^n = \frac{K_a Q_{c_{max}}^2}{H_{max}},\ K_c^n = \frac{K_c Q_{c_{max}}^2}{H_{max}},\ K^n = K_a^n + K_c^n \tag{45}$$

$$\alpha_a^n = \frac{\alpha_a Q_{c_{max}}}{H_{max}},\ \alpha_c^n = \frac{\alpha_c Q_{c_{max}}}{H_{max}},\ \alpha_n = \alpha_a^n + \alpha_c^n \tag{46}$$

$$\beta_c^n = \frac{\beta_c Q_{c_{max}}^2}{H_{max}} \tag{47}$$

with:

$$Q_{a_{max}} = Q_{c_{max}} = \sum_{i=1}^{k} Q_{i_{max}} \tag{48}$$

and

- H_{max} the maximum gross head, m;
- $Q_{i_{max}}$ the maximum flow rate of the i^{th} production generating unit, $m^3.s^{-1}$.

State model (41) then becomes:

$$\begin{cases} \alpha_a^n \dot{q_a} = z_b - z_e - K_a^n |q_a| q_a \\ \alpha_c^n \dot{q_c} = z_e - z_s - h_s - \beta_c^n {q_c}^2 - K_c^n |q_c| q_c \\ \dot{z_e} = \sigma(q_a - q_c) \end{cases} \tag{49}$$

where:

$$\sigma = \frac{Q_{c_{max}}}{H_{max} S_e} \tag{50}$$

On the other hand, equations (34), (36) and (38) become:

$$h = z_e - z_d - K_c^n |q_c| q_c - \alpha_c^n \dot{q_c} \tag{51}$$

$$h = z_s - z_d - h_s + \beta_c^n {q_c}^2 \tag{52}$$

$$h = z_b - z_d - K^n |q_c| q_c - \alpha_n \dot{q_c} \tag{53}$$

providing three different expressions for h.

Equation (51) will be preferred if both the height Z_e and the flow rate Q are known, while equation (52) relies on the pressure P_s^r and the flow rate Q. If neither of these two expressions can be used to compute h due to lack of required measurements, we may then rely on equation (53) keeping in mind that it is based on an additional simplifying assumption.

This quantity h is needed for the hydraulic power, which is obtained by:

$$P_h = \rho g H Q \tag{54}$$

where Q the flow rate turbinated/pumped by the considered generating unit, m^3/s.

When normalized, this becomes:

$$p_h = \gamma h q \tag{55}$$

with:

$$\gamma = \frac{\rho g Q_{max} H_{max}}{S_n},\ q = \frac{Q}{Q_{max}} \tag{56}$$

and Q_{max} the maximum flow turbined/pumped by the considered generating unit, m^3/s.

2.3 Hydromechanical Model

By combining the mechanical model and the hydraulic model (by injecting (55) into (22)), an overall hydromechanical model can be given by the following state representation:

$$\begin{cases} H_c \dot{e_c} = \eta \gamma h q - p_e - D(e_c - \sqrt{e_c}) \\ \omega = \sqrt{e_c} \end{cases} \tag{57}$$

where w is indeed usually measured in industrial plants, as well as driving variables p_e and q, while h can be obtained from (51), (52), or (53) as discussed before.

This model can also be written in the (approximate) standard form:

$$M \dot{\omega} = \eta \gamma h q - p_e - D(\omega - 1) \tag{58}$$

3. INDUSTRIAL-DATA-BASED VALIDATION

Let us illustrate and comment here the validity of models (57) and (58) when using industrial data collected on plants in real operation.

3.1 Model Comparison

As a first validation approach, both models (57) (kinetic model) and (58) (standard model) are simulated on the basis of industrial recordings of rotor speed w and driving powers (in short p_e and p_m).
Two cases are presented here:

• A first one with large disturbances, as they can be met in small electrical networks (as in islands). In that case, the models produce quite different results (Fig. 3), claiming for the choice of the kinetic model.

• A second one with small disturbances (most common in large networks): in that case the results with the two models do not allow to distinguish them clearly (Fig. 4).

The most suitable model can therefore be chosen depending on the stability of the network to which the synchronous generator is connected.

We can also compare here the three ways to calculate the net head (h) using (51), (52) and (53), with normalized parameters K_c^n and K^n taken from industrial measures, coefficient β_c^n and σ from known geometry, and all other variables from sensor data.
Results are presented in Figure 5, showing a good consistency, even though with some larger deviations when using the approximate version (52).

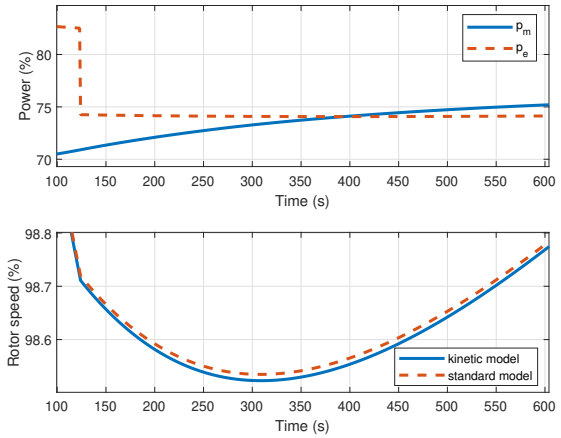

Fig. 3. Model comparison for a large disturbance

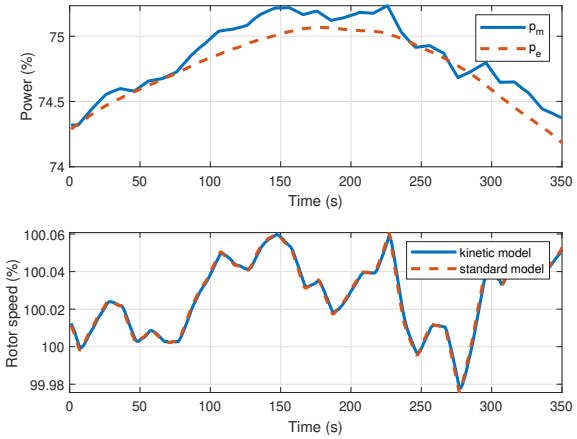

Fig. 4. Model comparison for small disturbances

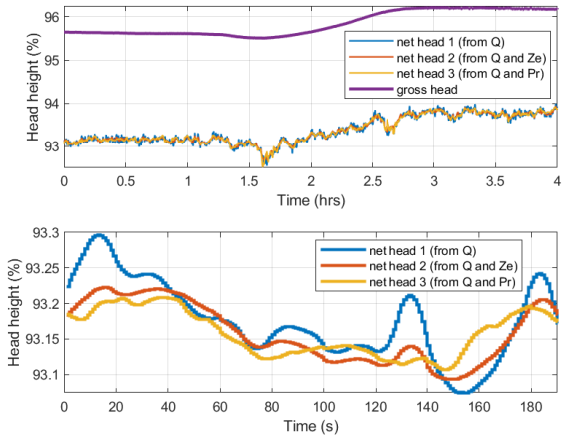

Fig. 5. (gross and net) head height (top), with time zoom (bottom).
n°1 is calculated with equation (53)
n°2 is calculated with equation (51)
n°3 is calculated with equation (52)

3.2 Parameter Identification

Let us here consider data from a large electrical network case, for which there is no big difference between kinetic and standard model. We can then consider model (58).

In order to estimate model parameters M, η and D, we can use Laplace transform so as to obtain the output as a function of the different inputs in the form of a sum of transfer functions ($Y = \sum_i H_i U_i$) :

$$\omega(s) = \frac{\eta}{Ms+D}\gamma hq(s) + \frac{1}{Ms+D}(-p_e(s)) + \frac{D}{Ms+D} \tag{59}$$

where $\omega(s)$, $hq(s)$, $p_e(s)$ stand for Laplace transforms of $\omega(t)$, $h(t)q(t)$, $p_e(t)$ respectively.
For the identification, ω, q and p_e are given by industrial measurements, while h is calculated from (52) using q, z_e and h_s (the pressure, see 6, the electrical power and the hydraulic power are filtered using a 2^{nd} order low pass filter without delay) which are industrial measures too. The other parameters like the section or the lenght of the headrace tunnel and the penstock are also known.

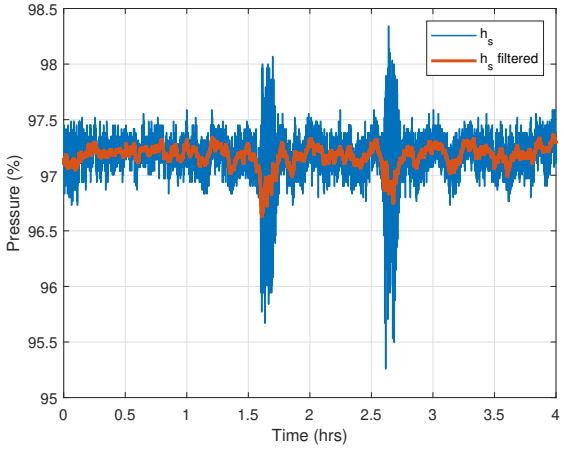

Fig. 6. Pressure h_s (raw and filtered)

We can then use the SRIVC-based (Simplified Refined Instrumental Variable method for Continuous-time systems) function from the CONTSID Matlab Toolbox (see Garnier and Gilson (2018)) to estimate these parameters.

On the other hand, normalized parameters K_c^n and K^n, entering in hydraulic model (49) and characteristic of some losses, can be estimated from equations (51), (52) and (53) as follows (see estimation results in Fig. 7):

$$K_c^n = \frac{1}{|q_c|q_c}(z_e - z_s + h_s - \alpha_c^n \dot{q}_c - \beta_c^n q_c^2) \tag{60}$$

$$K^n = \frac{1}{|q_c|q_c}(z_b - z_s + h_s - \alpha_n \dot{q}_c - \beta_c^n q_c^2) \tag{61}$$

(where $\dot{q}_c$ is estimated from measurement of q_c).

3.3 Model Validation

The model validation can be achieved by comparing the simulated output of the model when fed with industrial

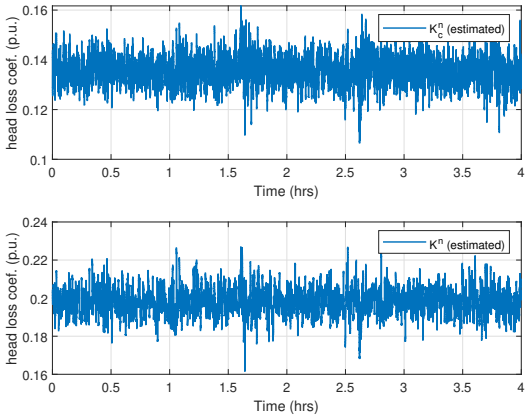

Fig. 7. Estimation of head loss coefficients K_c^n and K^n

data, to the corresponding industrial measurements. This is done here on the basis of identification results, both for hydraulic model (49), and for hydromechanical one (58). For the first one, q_c and z_e are shown in Figures 8 and 9 respectively, while ω is displayed for the second one, in Figure 10. They all show a pretty good accordance between simulation and measurements, which is quite promising for possible future monitoring purposes.

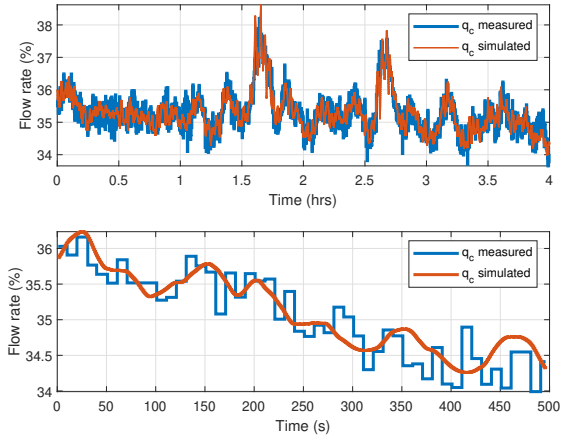

Fig. 8. Flow rate q_c (measured and simulated)

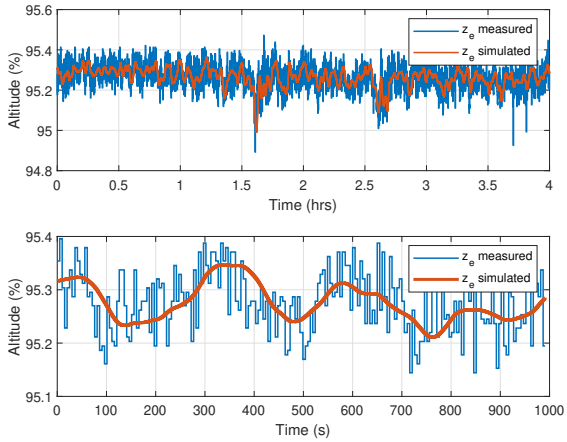

Fig. 9. Height z_e (measured and simulated)

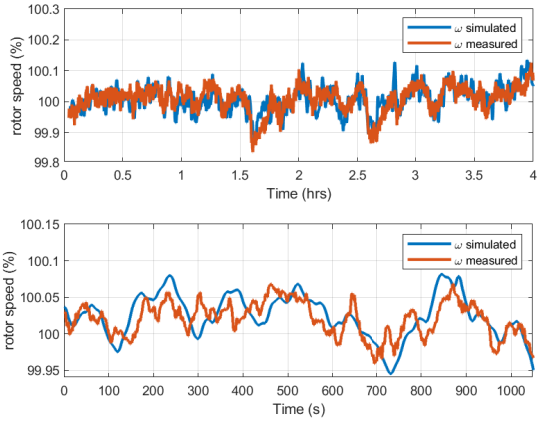

Fig. 10. Rotor speed ω measured and simulated

4. CONCLUSION

In this article, we have exhibited hydraulic and mechanical models that can be applied to hydroelectric power plants and that involve parameters whose knowledge at any time informs about the health of the studied plant. The models have been validated using measurements from sensors installed on operating plants. The results confirm the idea to push further the identification of the parameters in order to monitor them (for instance in the spirit of Robert and Besançon (2019)).

REFERENCES

Barret, P. (1987). *Régimes transitoires des machines tournantes électriques*. Eyrolles.

Bergen, A.R. and Vittal, V. (2000). *Power systems analysis*. Prentice Hall.

De Jaeger, E., Janssens, N., Malfliet, B., and Van De Meulebroeke, F. (1994). Hydro turbine model for system dynamic studies. *IEEE Transactions on Power Systems*, 9(4), 1709–1715.

Garnier, H. and Gilson, M. (2018). Contsid: a matlab toolbox for standard and advanced identification of black-box continuous-time models. *IFAC-PapersOnLine (18th SYSID, Stockholm, Sweden)*, 51(15), 688–693.

Gracino, R., Hansen, V., Goia, L., Campo, A., and Campos, B. (2021). System identification of a small hydropower plant. In *14th IEEE International Conference on Industry Applications*, 1430–1434. IEEE.

Machowski, J., Lubosny, Z., Bialek, J.W., and Bumby, J.R. (2020). *Power system dynamics: stability and control*. John Wiley & Sons.

Munoz-Hernandez, G.A., Jones, D.I., et al. (2012). *Modelling and controlling hydropower plants*. Springer Science & Business Media.

Ozkaya, D. and Kosalay, I. (2018). A review on system identification in power generation systems. *Commun. Fac. Sci. Univ. Ank. Series A2-A3*, 60(2), 147–162.

Robert, G. and Besançon, G. (2019). Fourier series-based kernel for frequency control performance monitoring of hydroelectric generating units. In *European Control Conference, Napoli, Italy*.

Robert, G. and Michaud, F. (2017). *Reduced order models for grid connected hydropower plants*, 49–77. Modeling and dynamic behaviour of hydropower plants (N. Kishor and J. Fraile-Ardanuy Eds), IET.